gemini-Porphyrazines: The Synthesis and Characterization of Metal-Capped *cis*- and *trans*-Porphyrazine Tetrathiolates

John W. Sibert,[†,§] Theodore F. Baumann,[†] David J. Williams,[‡] Andrew J. P. White,[‡] A. G. M. Barrett,*[,‡] and Brian M. Hoffman*[,†]

Contribution from the Department of Chemistry, Northwestern University, Evanston, Illinois 60208, and Department of Chemistry, Imperial College of Science, Technology and Medicine, South Kensington, London SW7 2AY, U.K.

Received June 7, 1996[⊗]

Abstract: Peripherally-functionalized porphyrazines of the form M[pz(A_n:B_{4-n})] (inset 1), where A and B symbolize functional moieties (e.g., a−d in Table 1) fused directly to the β-positions of the pyrroles, have the potential to serve in a wide range of applications. Previously, we reported the synthesis of porphyrazinedi- and octathiolate ligands, M[pz(b_3:c_1)] and M[pz(c_4)], respectively, where b is a fused benzo ring and c represents two thiolates fused at the β-pyrrole positions to form a dithiolene capable of the peripheral chelation of a metal ion. We describe here a general strategy that solves the more difficult problem of preparing and isolating the porphyrazinetetra- and hexathioethers and the porphyrazinetetra- and hexathiolates, with the focus being the trinuclear metal complexes of the *trans*- and *cis*-porphyrazinetetrathiolate isomers (*trans*- and *cis*-M[pz(b_2:d_2)]), denoted as *gemini* porphyrazines. Spectroscopic and electrochemical studies reveal that the physical properties of the *cis*- and *trans*-tetrathioether porphyrazines exhibit intriguing differences associated with their distinct molecular symmetries. These functionalized macrocycles have been used to prepare the *trans*- and *cis*-*gemini* porphyrazines **14** and **16**, the two isomeric porphyrazinetetrathiolate macrocycles that are peripherally-metalated with two bis(triethylphosphine)platinum(II) moieties. The X-ray structure of the *trans* isomer, **14**, is presented; it is the first structure of a porphyrazine or phthalocyanine having a *trans*-type substitution pattern.

Introduction

Peripherally-functionalized porphyrazines of the form, M[pz(A_n:B_{4-n})] (inset 1) where A and B symbolize functional groups (e.g., a−d in inset 1) fused directly to the β-positions of the pyrroles have the potential to exhibit novel magnetic and

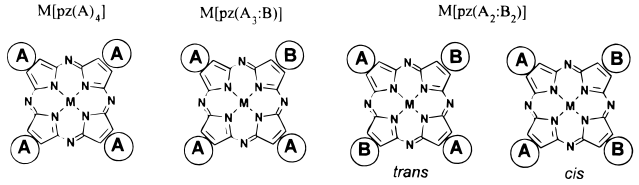

electronic properties and serve as building blocks in the assembly of higher order, metal-linked, multiporphyrinic arrays.[1] The preceding paper (*J. Am. Chem. Soc.* **1996**, *118*, 10479) describes the synthesis of unsymmetrical M[pz(A_1:B_3)] macrocycles,[2a] including the *solitaire*-porphyrazines[2] which have one metal ion bound to a single dithiolato chelation site at the porphyrazine periphery. We discuss here a strategy that solves the far harder problem of synthesizing and isolating both the *cis* and *trans*-M[pz(A_2:B_2)] macrocycles, and use this strategy to prepare the first trinuclear metal complexes of the *trans*- and *cis*-porphyrazine tetrathiolate isomers, the *gemini*-porphyrazines, **14** and **16** (inset 2).

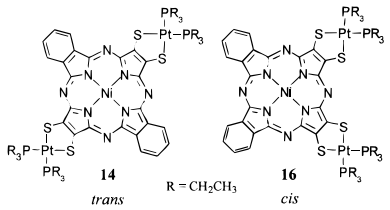

This synthesis of heterofunctionalized porphyrazines begins with the cocyclization of a pair of maleonitrile derivatives. Normally, it would be prohibitively difficult to isolate and purify each of the six possible porphyrazines produced in a cocyclization. The synthesis of the *solitaire*-porphyrazines described in the previous paper employed a procedure that yielded only M[pz(A_1:B_3)] and M[pz(B_4)] and that used reactants chosen so that only the former was soluble,[2] but this approach is not applicable to the preparation of the other mixed porphyrazines (inset 1). Instead, we have used a strategy that involves dinitrile pairs with groups A and B that have disparate polarities. As a result, even though the cyclization procedure produces all possible substituted porphyrazines as products, it is possible to chromatographically separate porphyrazines with different *n*, in particular the *cis* and *trans* $n = 2$ isomers, in acceptable yields. This permits the subsequent steps in the preparation of *gemini*-porphyrazines to be performed with chemically and isomerically pure reactants. As an illustration, we report the synthesis of the $n = 2$ and 3 porphyrazines, **8**−**10** (Table 1), as well as the preparation of the trimetallic *gemini*-porphyrazines,

[†] Northwestern University.
[‡] Imperial College of Science, Technology and Medicine.
[§] Present address: Department of Chemistry, East Carolina University, Greenville, NC 27858-4353.

[⊗] Abstract published in *Advance ACS Abstracts,* October 1, 1996.

(1) For alternative designs of multi-porphyrinic arrays, see: (a) Hanan, G. S.; Arana, C. R.; Lehn, J.-M.; Fenske, D. *Angew Chem., Int. Ed. Engl.* **1995**, *34*, 1122−1124. (b) Seth, J.; Palaniappan, V.; Johnson, T. E.; Prathapan, S.; Lindsey, J. S.; Bocian, D. F. *J. Am. Chem. Soc.* **1994**, *116*, 10578−10592. (c) Anderson, H. L. *Inorg. Chem.* **1994**, *33*, 972−981. (d) Lin, V. S.-Y.; Dimagno, S. G.; Therien, M. J. *Science* **1994**, *264*, 1105−1111. (e) Crossley, M. J.; Burn, P. L. *J. Chem. Soc., Chem. Commun.* **1991**, 1569−1571.

(2) (a) Baumann, T. F.; Nasir, M. S.; Sibert, J. W.; White, A. J. P.; Olmstead, M. M.; Williams, D. J.; Barrett, A. G. M.; Hoffman, B. M. *J. Am. Chem. Soc.* preceding paper (*J. Am. Chem. Soc.* **1996**, *118*, 10479). (b) Baumann, T. F.; Sibert, J. W.; Olmstead, M. M.; Barrett, A. G. M.; Hoffman, B. M. *J. Am. Chem. Soc.* **1994**, *116*, 2639−2640.

S0002-7863(96)01912-9 CCC: $12.00

Table 1. Compounds Prepared in This Study

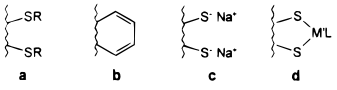

compd	M	pz(A_n:B_{4-n})
3	2H	pz(a)$_4$
4	2H	pz(a_3:b)
5	2H	*trans*-pz(a_2:b_2)
6	2H	*cis*-pz(a_2:b_2)
7	2H	pz(a:b_3)
8	Ni	pz(a_3:b)
9	Ni	*trans*-pz(a_2:b_2)
10	Ni	*cis*-pz(a_2:b_2)
11	Mn	*trans*-pz(a_2:b_2)
12	Mn	*cis*-pz(a_2:b_2)
13	Ni	*trans*-pz(c_2:b_2)
14	Ni	*trans*-pz(d_2:b_2) (M = Pt, L = $(PEt_3)_2$)
15	Ni	*cis*-pz(c_2:b_2)
16	Ni	*cis*-pz(d_2:b_2) (M = Pt, L = $(Pet_3)_2$)

14 and **16** (inset 2). The characterization of these molecules includes the X-ray structure determination of **14**, the first one of a porphyrazine *or* phthalocyanine having a *trans*-type substitution pattern.[3]

Materials and Methods

THF was distilled from sodium benzophenone ketyl. All other solvents were reagent grade and used as supplied. Anhydrous ammonia (Linde Specialty Gases) was ultra-high-purity grade. 1,2-Dicyanobenzene, **1**, was purchased from Aldrich and used as received. 2,3-Di-[(4-butyloxycarbonylbenzyl)thio]-2*Z*-butenedinitrile ((BCB)$_2$mnt), **2**, was prepared as reported.[2a] All other reagents were used as supplied without further purification. Radial chromatography was performed on a Chromatotron (Model 7924T), Harrison Research, Palo Alto, CA. The chromatotron plates were coated with Merck silica gel (TLC grade 7749 with gypsum binder).

^{1}H and ^{31}P NMR spectra were obtained using a Gemini 300 spectrometer. The ^{31}P NMR spectra were referenced using a 5% H_3PO_4 external reference. Electronic spectra were recorded using a Hewlett-Packard HP8452A spectrophotometer. Cyclic voltammetry experiments were performed at room temperature in freshly-distilled methylene chloride with 0.1 M tetrabutylammonium hexafluorophosphate as the supporting electrolyte using a Cypress Systems 2000 electroanalytical system. A platinum working electrode and Ag/AgCl reference electrode were used with ferrocene as an internal calibrant. Fast-atom bombardment mass spectra (FAB-MS) were obtained by Dr. Doris Hung using a VG-70-250E instrument. Elemental analyses were performed by Searle Laboratories, Skokie, IL and Oneida Research Services, Whitesboro, NY (supporting information, Table 1).

Synthesis of H$_2$[pz(a_n:b_{4-n})]. Magnesium metal (0.064 g, 0.0027 mol) was added to butanol (16 mL), and the solution was heated to reflux. A small chip of iodine was added to initiate the formation of the magnesium butoxide suspension. After 16 h, 1,2-dicyanobenzene (0.50 g, 0.004 mol) and (BCB)$_2$mnt (2.04 g, 0.004 mol) were simultaneously added to the solution. The reaction was heated at reflux for 24 h under a N_2 atmosphere. The butanol was removed under vacuum, and the crude reaction mixture dissolved in $CHCl_3$. The blue-green mixture was filtered to remove the insoluble Mg(pc) formed as a byproduct in the cyclization. After concentration on a rotary evaporator, the filtrate was passed through a silica column (1−2% MeOH/$CHCl_3$ as eluent) which removed non-porphyrazine byproducts and afforded all of the Mg-porphyrazines as a mixture. Isolation of the Mg-porphyrazines was achieved by chromatography using the Chromatotron (1 or 2 mm plate; 0.5−1% MeOH/CH_2Cl_2 as eluent). This method, however, worked poorly due to the formation of broad chromatographic bands and did not produce analytically pure products. A better approach begins with the demetalation of the entire mixture of Mg-porphyrazines by overnight treatment with trifluoroacetic acid (30 mL) prior to separation of the individual porphyrazines. The resulting blue solution was poured into ice water (300 mL) and stirred, causing the immediate formation of a precipitate. Following neutralization with concentrated NH_4OH, the solid was collected by filtration and washed thoroughly with water, MeOH, and a small amount of Et_2O. The crude product was dissolved in a minimum of CH_2Cl_2 and chromatographed using the Chromatotron (1 or 2 mm plate; 0−0.5% MeOH/CH_2Cl_2 as eluent). Each of the porphyrazine products was collected in the order listed below.

2,3,7,8,12,13,17,18-Octakis[(4-butyloxycarbonylbenzyl)thio]porphyrazine, H$_2$[pz(a_4)], 3. This porphyrazine was collected as the first purplish-blue band to elute. No attempt was made at determining a yield for this compound: ^{1}H NMR ($CDCl_3$) δ (ppm) 7.70 (d, 16H, ar (benzyl)), 7.34 (d, 16H, ar (benzyl)), 5.15 (s, 16H, ArC*H*$_2$-), 4.21 (t, 16H, -C*H*$_2$O), 1.67 (qn, 16H, -OCH$_2$C*H*$_2$-), 1.40 (sx, 16H, -C*H*$_2$CH$_3$), 0.90 (t, 24H, -CH$_2$C*H*$_3$), −3.10 (s, 2H, N*H*); UV-vis($CHCl_3$) λ_{max} 354, 508, 648, 716 nm; FAB-MS 2113 (M + H$^+$).

2,3,7,8,12,13-Hexakis[(4-butyloxycarbonylbenzyl)thio]-17,18-benzoporphyrazine, H$_2$[pz(a_3:b)], 4. This blue porphyrazine was collected as the second band to elute from the Chromatotron. Recrystallization from CH_2Cl_2/MeOH yielded a microcrystalline product (160 mg; 7%): ^{1}H NMR ($CDCl_3$) δ (ppm) 8.76 (m, 2H, ar (fused benzo)), 8.05 (m, 2H, ar (fused benzo)), 7.80 (m, 12H, ar (benzyl)), 7.34 (m, 12H, ar (benzyl)), 5.24 (s, 4H, ArC*H*$_2$-), 5.13 (s, 4H, ArC*H*$_2$-), 5.08 (s, 4H, ArC*H*$_2$-), 4.21 (t, 12H, -C*H*$_2$O), 1.65 (qn, 12H, -OCH$_2$C*H*$_2$-), 1.39 (sx, 12H, -C*H*$_2$CH$_3$), 0.90 (t, 18H, -CH$_2$C*H*$_3$), −2.90 (s, 2H, N*H*); UV/vis-($CHCl_3$) λ_{max} 356, 500, 624, 680, 726 nm; FAB-MS 1698 (M + H$^+$).

2,3,12,13-Tetrakis[(4-butyloxycarbonylbenzyl)thio]-7,8;17,18-dibenzporphyrazine, **H$_2$[*trans*-pz(a_2:b_2)], 5.** This purplish-pink porphyrazine was the third band to elute from the Chromatatron. Recrystallization from CH_2Cl_2/MeOH yielded a microcrystalline product (130 mg; 5%); ^{1}H NMR ($CDCl_3$) δ (ppm) 8.61 (m, 4H, ar (fused benzo)), 7.89 (m, 4H, ar (fused benzo)), 7.80 (d, 8H, ar (benzyl)), 7.34 (d, 8H, ar (benzyl)), 5.28 (s, 8H, ArC*H*$_2$-), 4.16 (t, 8H, -C*H*$_2$O), 1.63 (qn, 8H, -OCH$_2$C*H*$_2$-), 1.38 (sx, 8H, -C*H*$_2$CH$_3$), 0.90 (t, 12H, -CH$_2$C*H*$_3$), -3.36 (s, 2H, N*H*); UV/vis(CH_2Cl_2) λ_{max} 350, 590, 708, 747 nm; FAB-MS 1304 (M + H$^+$).

2,3,7,8-Tetrakis[(4-butyloxycarbonylbenzyl)thio]-12,13;17,18-dibenzporphyrazine, H$_2$[*cis*-pz(a_2:b_2)], 6. This blue porphyrazine was isolated as the fourth band to elute from the Chromatotron. Recrystallization from CH_2Cl_2/MeOH yielded a microcrystalline product (285 mg; 11%): ^{1}H NMR ($CDCl_3$) δ (ppm) 8.55 (m, 4H, ar (fused benzo)), 7.91 (m, 4H, ar (fused benzo)), 7.79 (m, 8H, ar (benzyl)), 7.45 (d, 4H, ar (benzyl)), 7.36 (d, 4H, ar (benzyl)), 5.11 (s, 4H, ArC*H*$_2$-), 5.06 (s, 4H, ArC*H*$_2$-), 4.18 (m, 8H, -C*H*$_2$O), 1.62 (m, 8H, -OCH$_2$C*H*$_2$-), 1.37 (m, 8H, -C*H*$_2$CH$_3$), 0.89 (m, 12H, -CH$_2$C*H*$_3$), −2.40 (s, 2H, N*H*); UV/vis(CH_2Cl_2) λ_{max} 352, 628, 652, 692 nm; FAB-MS 1304 (M + H$^+$).

2,3-Bis[(4-butyloxycarbonylbenzyl)thio]norphthalocyanine, H$_2$[pz(a:b_3)], 7. This blue porphyrazine was the fifth and final band collected from the Chromatatron. Characterization of this compound was as previously reported.[4]

Synthesis of [2,3,7,8,12,13-Hexakis[(4-butyloxycarbonylbenzyl)thio]-17,18-benzporphyrazinato]nickel(II) Ni[pz(a_3:b)], 8. Metal-free **4** (0.200 g, 0.12 mmol), anhydrous Ni(OAc)$_2$ (0.21 g, 1.2 mmol), chlorobenzene (10 mL), and DMF (5 mL) were heated to 100 °C under nitrogen for 5 h. Following removal of the solvent under vacuum, the product was washed with 5% HCl in MeOH, pure MeOH, and then Et_2O. Recrystallization from CH_2Cl_2/MeOH yielded microcrystalline product in near quantitative yield: ^{1}H NMR ($CDCl_3$) δ (ppm) 8.68 (m, 2H, ar (fused benzo)), 8.00 (m, 2H, ar (fused benzo)), 7.78 (m, 12H, ar (benzyl)), 7.32 (m, 12H, ar (benzyl)), 5.08 (s, 4H, ArC*H*$_2$-), 5.06 (s, 4H, ArC*H*$_2$-), 5.02 (s, 4H, ArC*H*$_2$-), 4.21 (t, 12H, -C*H*$_2$O), 1.66 (qn, 12H, -OCH$_2$C*H*$_2$-), 1.39 (sx, 12H, -C*H*$_2$CH$_3$), 0.92 (t, 18H, -CH$_2$C*H*$_3$); UV/vis($CHCl_3$) λ_{max} 326, 644, 682 nm; FAB-MS 1755 (M + H$^+$).

Synthesis of [2,3,12,13-Tetrakis[(4-butyloxycarbonylbenzyl)thio]-7,8;17,18-dibenzoporphyrazinato] nickel(II), Ni[*trans*-pz(a_2:b_2)], 9. Porphyrazine **9** was prepared from **5** by an identical procedure to that used in the preparation of **8**. Recrystallization from CH_2Cl_2/MeOH yielded microcrystalline product in near quantitative yield: ^{1}H NMR

(3) For examples of unsymmetrical phthalocyanines having a *trans*-type substitution pattern without crystal structures, see: (a) Kobayashi, N.; Ashida, T.; Osa, T.; Konami, H. *Inorg. Chem.* **1994**, *33*, 1735−1740. (b) Kobayashi, N.; Ashida, T.; Osa, T. *Chem. Lett.* **1992**, 2031−2034. (c) Ikeda, Y.; Konami, H.; Hatano, M.; Mochizuki, K. *Chem. Lett.* **1992**, 763−766.

(4) (a) Schramm, C. S.; Hoffman, B. M. *Inorg. Chem.* **1980**, *19*, 383−385. (b) Linstead, R. P.; Whalley, M. *J. Chem. Soc.* **1952**, 4839−4846.

($CDCl_3$) δ (ppm) 8.42 (m, 4H, ar (fused benzo)), 7.80 (m, 12H, ar (fused benzo, benzyl)), 7.36 (d, 8H, ar (benzyl)), 5.04 (s, 8H, ArCH_2-), 4.22 (t, 8H, -CH_2O), 1.67 (qn, 8H, -OCH$_2$CH_2-), 1.38 (sx, 8H, -CH_2-CH$_3$), 0.92 (t, 12H, -CH$_2$CH_3). Uv/vis(CH_2Cl_2) λ_{max} 354, 605, 722 nm; FAB-MS 1360 (M + H$^+$).

Synthesis of [2,3,7,8-Tetrakis[(4-butyloxycarbonylbenzyl)thio]-12,13;17,18-dibenzporphyrazinato]nickel(II), Ni[*cis*-pz(a$_2$:b$_2$)], 10. Porphyrazine **10** was prepared from **6** by an identical procedure to that used in the preparation of **8**. Recrystallization from CH_2Cl_2/MeOH yielded microcrystalline product in near quantitative yield: ^{1}H NMR ($CDCl_3$) δ (ppm) 8.21 (m, 4H, ar (fused benzo)), 7.81 (m, 8H, ar (benzyl)), 7.69 (m, 4H, ar (fused benzo)), 7.40 (d, 4H, ar (benzyl)), 7.33 (d, 4H, ar (benzyl)), 5.00 (s, 4H, ArCH_2-), 4.97 (s, 4H, ArCH_2-), 4.20 (m, 8H, -CH_2O), 1.64 (m, 8H, -OCH$_2$CH_2-), 1.38 (m, 8H, -CH_2-CH$_3$), 0.90 (t, 12H, -CH$_2$CH_3). UV/vis(CH_2Cl_2) λ_{max} 336, 602, 659 nm; FAB-MS 1360 (M + H$^+$).

Synthesis of [2,3,12,13-Tetrakis[(4-butyloxycarbonylbenzyl)thio]-7,8;17,18-dibenzporphyrazinato]-chloromanganese(III), MnCl-[*trans*-pz(a$_2$:b$_2$)], 11. Metal-free **5** (0.200 g, 0.12 mmol), excess $MnCl_2$, chlorobenzene (10 mL), and DMF (5 mL) were heated to 100 °C under nitrogen for 5 h. Following removal of the solvent under vacuum, the product was washed with water MeOH and then ethyl ether. Purification by silica gel chromatography (4% MeOH/CH_2Cl_2) produced **11** as a green solid in near quantitative yield: UV/vis(CH_2Cl_2) λ_{max} 382, 654, 780 nm; FAB-MS 1356 (M − Cl$^-$).

Synthesis of [2,3,7,8-Tetrakis[(4-butyloxycarbonylbenzyl)thio]-12,13;17,18-dibenzoporphyrazinato]chloromanganese(III), MnCl-[*cis*-pz(a$_2$:b$_2$)], 12. Porphyrazine **12** was prepared from **6** by an identical procedure to that used in the preparation of **11**. The product was isolated by silica gel chromatography (4% MeOH/CH_2Cl_2) as a brown oily solid in near quantitative yield: UV/vis(CH_2Cl_2) λ_{max} 357, 473, 712 nm; FAB-MS 1356 (M − Cl$^-$).

Synthesis of Sodium [7,8;17,18-dibenzporphyrazinato]nickel(II)-2,3,12,13-tetrathiolate, Ni[*trans*-pz(c$_2$:b$_2$)], 13. Schlenk techniques were used in this step. Compound **9** (0.100 g, 0.074 mmol) was suspended in a solution of liquid NH_3 (25 mL) at −78 °C. Socium metal (0.027 g, 1.18 mmol) was freshly cut under hexanes and added to the suspension. Once the sodium dissolved, THF (10 mL) was added to solubilize the porphyrazine. The solution was allowed to reflux at −33 °C for 30 min, whereupon the solution turned purple and then green. Following the addition of ammonium chloride (0.031 g, 0.6 mmol), solvent was evaporated under a stream of argon, yielding a fine blue powder containing sodium chloride and the sodium salt of the tetrathiolate. Due to the air-sensitive nature of this solid, no attempt was made to isolate the product.

Synthesis of Ni[*trans*-pz(b$_2$:d$_2$)] (M = Pt,L = (PEt$_3$)$_2$), 14. To the deep blue solution of crude tetrathiolate **13** in deaerated MeOH (30 mL) was added $(Et_3P)_2PtCl_2$ (0.074 g, 0.148 mmol). After 30 min, the blue precipitate that formed was collected by filtration under ambient conditions. The product was dissolved in CH_2Cl_2 and chromatographed on silica gel using 2% MeOH in CH_2Cl_2 as the eluent. The major purple band was collected to yield product **14** (45 mg; 40% based on **9**). X-ray diffraction quality, cube-shaped crystals were grown by slow evaporation of a CH_2Cl_2 solution in the presence of 1,2-dichlorobenzene: ^{1}H NMR (CD_2Cl_2) δ (ppm) 9.39 (m, 4H, ar (fused benzo)), 8.22 (m, 4H, ar (fused benzo)), 2.40 (m, 24H, -CH_2CH$_3$), 1.36 (m, 36H, -CH$_2$CH_3); ^{31}P NMR (CD_2Cl_2, H_3PO_4 external reference) δ (ppm) 7.33 (J_{Pt-P} = 2708 Hz); UV/vis(CH_2Cl_2) λ_{max} 330, 568, 600, 676 nm; FAB-MS 1457 (M + H$^+$).

Synthesis of Sodium [12,13;17,18-dibenzporphyrazinato]nickel-(II)-2,3,7,8-tetrathiolate, Ni[*cis*-pz(b$_2$:c$_2$)], 15. Complex **10** (0.100 g, 0.074 mmol) was deprotected by the method described above for compound **13**. Again, due to the air-sensitive nature of the tetrathiolate, no attempt was made to isolate the product.

Synthesis of Ni[*cis*-pz(b$_2$:d$_2$)] (M = Pt,L = (PEt$_3$)$_2$), 16. To the blue solution of crude tetrathiolate **15** in deaerated MeOH (30 mL) was added $(Et_3P)_2PtCl_2$ (0.074 g, 0.148 mmol). After 30 min, the blue-green precipitate that formed was collected by filtration under ambient conditions. The product was dissolved in CH_2Cl_2 and chromatographed on silica gel using 2% MeOH in CH_2Cl_2 as the eluent. The major aqua-blue band was collected to yield product **16** (45 mg; 40% based on **10**). Crystallization by slow diffusion of methanol into a CH_2Cl_2 solution produced **16** as blue needles: ^{1}H NMR (CD_2Cl_2) δ (ppm) 9.36 (m, 4H, ar (fused benzo)), 8.11 (m, 4H, ar (fused benzo)), 2.40 (m, 24H, -CH_2CH$_3$), 1.37 (m, 36H, -CH$_2$CH_3); ^{31}P NMR (CD_2Cl_2, H_3PO_4 external reference) δ (ppm) 7.23, 6.82 (J_{Pt-P} = 2704 Hz, J_{P-P} = 23 Hz); UV/vis(CH_2Cl_2) λ_{max} 328, 604, 680 nm; FAB-MS 1457 (M + H$^+$).

Table 2. Crystallographic Data for **14**

chem formula	$C_{48}H_{68}N_8NiP_4Pt_2S_4\cdot 2[C_6H_4Cl_2]$
fw	1752.1
crystal system	monoclinic
space group	$P2_1/c$
a, Å	13.006(4)
b, Å	18.645(8)
c, Å	14.469(6)
β, deg	105.86(3)
V, Å^3	3375(2)
Z[a]	2
T, K	293(2)
λ(Cu Kα), Å	1.54178
ρ_{calcd}, g/cm^3	1.72
μ, cm^{-1}	117.8
GOF[b] on F^2	1.039
final R indices[c] [$I > 2\sigma(I)$]	R_1 = 0.0350, wR_2 = 0.0848

[a] The molecule has crystallographic C_i symmetry. [b] [b]$GOF = [\sum[w(F_o^2 - F_c^2)^2]/(M - N)]^{1/2}$ where M is the number of reflections and N is the number of parameters refined. [c] $R_1 = \sum||F_o| - |F_c||/\sum|F_o|$; $wR_2 = [\sum[w(F_o^2 - F_c^2)^2]/\sum[w(F_o^2)^2]]^{1/2}$.

Scheme 1[a]

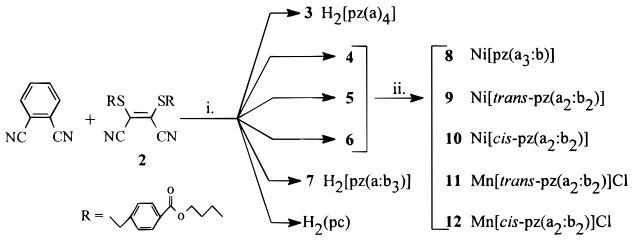

[a] i. (a) Mg(OBu)$_2$, BuOH, 120 °C (b) CF_3COOH. ii. M(II)X$_2$ (M = Ni, Mn; X = OAc, Cl) DMF, PhCl, 100 °C.

Structure Determination for *gemini*-Porphyrazine 14. Single-crystal X-ray diffraction data for **14** were collected using a Siemens P4/RA diffractometer with Cu-Kα radiation (graphite monochromator) using ω-scans. A bronze irridescent rhombahedron of dimensions 0.11 × 0.07 × 0.07 mm was used. Crystallographic data and refinement parameters are summarized in Table 2. The structure was solved by direct methods, and all the non-hydrogen atoms of the complex were refined anisotropically. The *o*-dichlorobenzene solvent was highly disordered (three overlapping, partial occupancy orientations were identified), and only the chlorine atoms of the two major occupancy optimized molecules were refined anisotropically. Full-matrix least-squares refinement based on F^2 gave R_1 = 0.035, wR_2 = 0.085 for 4294 independent observed reflections [$|F_o| > 4\sigma(|F_o|)$, $2\theta^2$ 120°] and 374 parameters.

Results and Discussion

Synthesis of the *gemini*-Porphyrazine Complexes. As illustrated in Scheme 1, preparation of the n = 2 and 3 peripherally-functionalized porphyrazines begins with the Mg(II) template cyclization[4] of a pair of maleonitrile derivatives, **1** and **2** in this case, to yield a mixture of macrocycles. To prepare peripherally metalated porphyrazines this is followed by purification of the desired protected mixed porphyrazine, thiolate deprotection, and peripheral chelation of a metal complex. The cyclization step, unlike the equivalent one in the synthesis of *solitaire*-porphyrazines,[2] is nonspecific, producing all six possible porphyrazine products with n = 0−4 dithioether moieties (inset 1) incorporated into the macrocycle, including the *cis* and *trans* isomers of the n = 2 porphyrazine. The use of a pair of dinitriles that have different polarities,[5] such as **1** and **2** not only permits separation of porphyrazines

with different *n*, but further allows for the separation of the *cis* and *trans* geometries of the $n = 2$ porphyrazine macrocycles. The $n = 2$ porphyrazines in the *trans* geometry have no net dipole and quickly elute from silica gel. In the *cis* geometry the dipole moments of the pyrroles of one type add vectorially, the molecules are relatively polar and, thus, elute from silica gel more slowly. In general, the greater the disparity (or opposition) in polarity of the peripheral substituents on the porphyrazine, the better the chromatographic separation of the six porphyrazine products and, in particular, of the two $n = 2$ isomers.

Commercially available phthalonitrile, **1**, was a cheap and convenient choice as the nonpolar dinitrile for development of this strategy. The protected dithiomaleonitrile derivative, **2**, where R = 4-butyloxycarbonylbenzyl (BCB) was chosen as the polar protecting group because it is easily prepared,[2a] robust to the cyclization conditions, readily subject to reductive cleavage, and enhances the solubility of the porphyrazine products. Template cyclization of equimolar quantities of **1** and **2** produces all six porphyrazine products (Scheme 1). Of these, Mg(pc) was trivially separated from the other five because it is relatively insoluble in ordinary organic solvents. The remaining Mg-[porphyrazines] were demetalated with trifluoroacetic acid to remove the Mg(II) ion, a step that facilitates further separations. The free-base macrocycles, **3**−**7**, were isolated individually by radial chromatography. The *trans*- and cis- protected porphyrazines, **5** and **6**, were obtained in 5% and 11% yields, respectively; the $n = 3$ macrocycle, **4**, was obtained in 8% yield. Subsequently, **4**−**6** were each treated with $Ni(OAc)_2$ and/or $MnCl_2$ producing the metalated BCB-protected porphyrazines, **8**−**12**, in nearly quantitative yields.[6]

Reductive debenzylation of **9** and **10**, carried out with sodium metal in liquid ammonia/THF produced, respectively, the *cis*- and *trans*-porphyrazine tetrathiolates, **13** and **15**, as dark-blue solutions in MeOH. The tetrathiolates were then treated individually with $(Et_3P)_2PtCl_2$ to yield the trinuclear metal complexes **14** and **16**.

^{1}H NMR Studies of the Unsymmetrical Porphyrazines, H_2[pz(a$_n$:b$_{4-n}$)], 3−7. Proton NMR spectroscopy played a key role in distinguishing the unsymmetrically substituted porphyrazines, **3**−**7**, with the clearest distinction observed in the region $\delta = 4.0-6.0$ ppm. The resonances in this region are assigned to the methylene protons of the BCB-protecting group (-C**H**$_2$-C_6H_4-CO_2C**H**$_2$-$(CH_2)_2CH_3$) and clearly reveal the molecular symmetry of a given porphyrazine. For example, the ^{1}H NMR spectrum of the D_{4h} symmetric porphyrazine **3** ($n = 4$) contains one triplet (-CO_2C**H**$_2$-) and one singlet (S-C**H**$_2$-C_6H_4-) at $\delta =$ 4.21 and 5.15 ppm, respectively, since all eight BCB moieties are chemically equivalent. The spectrum of the C_{2v} symmetric $n = 3$ porphyrazine **4** contains a broadened triplet ($\delta = 4.21$ ppm) and three distinct singlets ($\delta = 5.08$, 5.13, and 5.24 ppm) corresponding to the three chemically inequivalent BCB-protecting groups. The spectrum of the D_{2h} symmetric *trans* macrocycle **5** exhibits just one triplet ($\delta = 4.16$) and one singlet ($\delta = 5.28$) because the four BCB groups are equivalent. This pattern is doubled in the cis macrocycle **6** (C_{2v}) whose spectrum contains a multiplet ($\delta = 4.18$) and two distinct singlets ($\delta =$ 5.06 and 5.11). Finally, the C_{2v} symmetry of porphyrazine **7** ($n = 1$) leads to a spectrum with only one triplet and one singlet.[2a] The aromatic region of the proton spectra for **3**−**7** contain signals from the protons of the para-substituted benzyl groups and the fused benzo rings. Although these resonances overlap such that analysis is more difficult, they, nonetheless, show splitting patterns consistent with the various symmetries of the macrocycles.

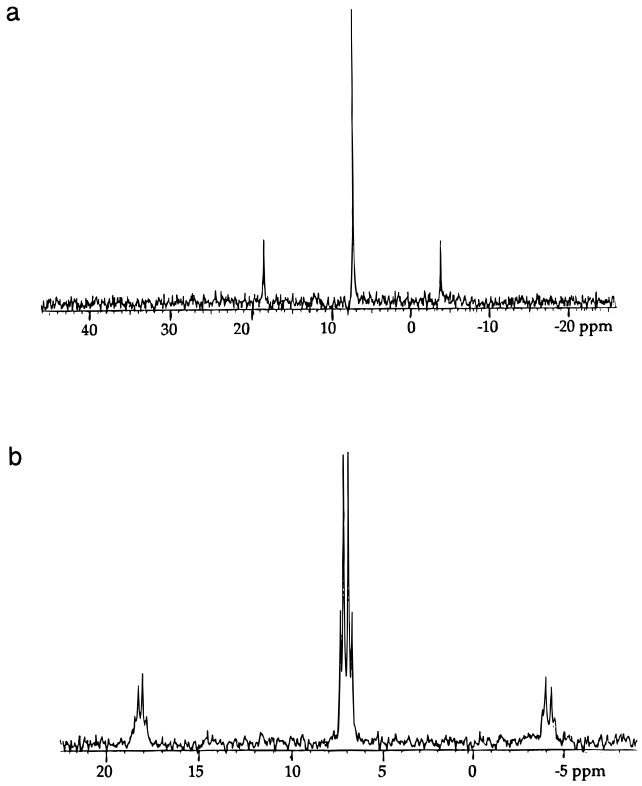

Figure 1. ^{31}P NMR spectra of *gemini*-porphyrazines **14**, a, and **16**, b, in CD_2Cl_2.

Table 3. ^{31}P NMR Chemical Shifts and Coupling Constants for *gemini*-Porphyrazines **14** and **16** and Related Complexes[a]

compd	δ (ppm)	J_{Pt-P} (Hz)	J_{P-P} (Hz)
14	7.33(s)	2708	
$Pt(PEt_3)_2$(mnt)[7a]	4.82(s)	2749	
16	7.32(d)	2704	23
	6.82(d)	2704	23
$Pt(PPh_3)_2$(ecda)[7b]	19.04(d)	1577	22.1
	18.35(d)	1500	22.1

[a] ^{31}P NMR spectra were taken in dichloromethane-*d*. Chemical shifts reported in ppm relative to 5% H_3PO_4−D_2O.

In addition, spectra of each of the free-base porphyrazines, **3**−**7**, contain singlets between −2.0 and −3.5 ppm which are assigned to the internal pyrrole protons.

^{31}P NMR Studies of the Trimetallic *cis*- and *trans-gemini*-Porphyrazines, 14 and 16. The molecular symmetries of the *cis*- and *trans-gemini*-porphyrazines, **14** and **16**, are clearly manifest in their ^{31}P NMR spectra (Figure 1); the ^{31}P NMR chemical shifts and coupling constants are listed in Table 3. The four peripheral phosphine ligands of the D_{2h}-symmetric *trans* complex, **14**, are all symmetry-equivalent, and, thus, the ^{31}P NMR spectrum contains three peaks centered at 7.33 ppm. The central line is from $[Pt(PEt_3)_2]^{2+}$ moieties containing isotopes of platinum with $I = 0$ (67% abundance). The flanking doublet results from $[^{195}Pt(PEt_3)_2]^{2+}$ (^{195}Pt: $I = 1/2$; 33% abundance); the magnitude of the doublet splitting (J_{Pt-P}) is 2708 Hz. In contrast, for the C_{2v}-symmetric *cis* complex **16** the triethylphosphine ligands in $[Pt(PEt_3)_2]^{2+}$ are symmetry-inequivalent. Thus, the ^{31}P NMR spectrum of **16** contains doublets at 6.82 and 7.23 ppm for the two types of phosphorus atoms associated with the $I = 0$ isotopes of platinum; the magnitude of the coupling constant (J_{P-P}) is 23 Hz. The non-first-order spectrum arises from the similarity in magnitude of

(5) A similar strategy has been used to prepare an unsymmetrically substituted phthalocyanine. Linβen, T. G.; Hanack, M. *Chem. Ber.* **1994**, *127*, 2051−2057.

(6) Velazquez, C. S.; Fox, G. A.; Broderick, W. E.; Andersen, K.; Anderson, O. P.; Barrett, A. G. M.; Hoffman, B. M. *J. Am. Chem. Soc.* **1992**, *114*, 7416−7424.

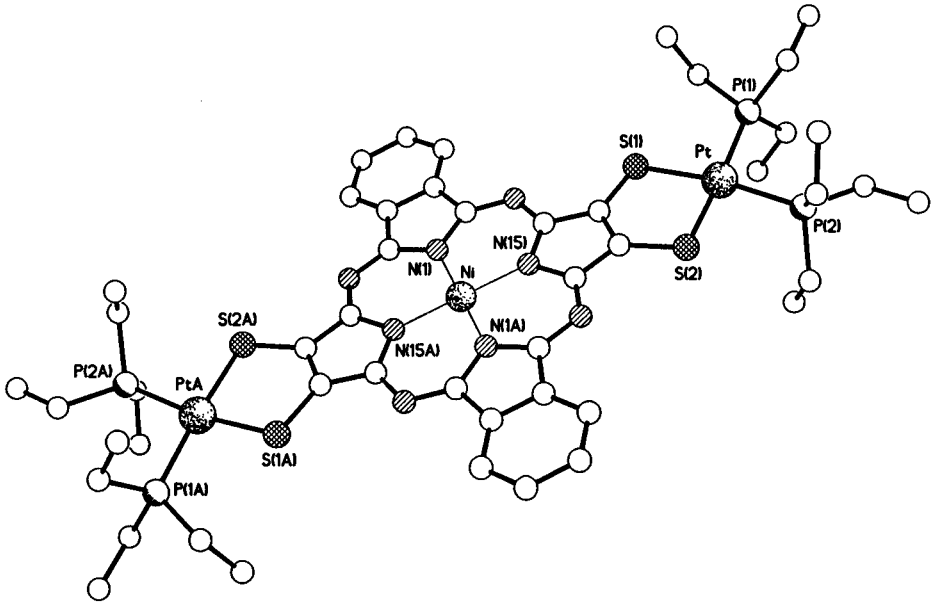

Figure 2. X-ray structure of **14** with hydrogen atoms omitted for clarity.

the coupling constant, J_{P-P}, and the chemical shift difference between the two types of P atoms. The splitting pattern is repeated in the ^{195}Pt satellites, where $J_{Pt-P} = 2704$ Hz. The two types of P atoms in principle should couple differently with the ^{195}Pt center, but this is not observed in the spectrum of **16**. Apparently, the two coupling constants (J_{Pt-P}) are too nearly equal to be distinguishable. The ^{31}P chemical shifts and coupling constants are similar to those reported for analogous square-planar Pt(II) complexes with *cis*-diphosphine ligands and both symmetrical and unsymmetrical dithiolene ligands (Table 3).[7]

X-ray Crystal Structure of *trans-gemini*-Porphyrazine 14. X-ray quality crystals of **14**, the *trans-gemini*-porphyrazine that contains a centrally-bound Ni(II) ion and two $[Pt(PEt_3)_2]^{2+}$ moieties coordinated to the periphery in a *trans* geometry, were grown from CH_2Cl_2/dichlorobenzene. The structure is shown in Figure 2. Table 4 presents selected symmetry averaged bond distances and bond angles for **14**, M(pc),[8] and Ni[pz(d)$_4$][9] where M = Ni, L = (1,1′-diphenylphosphino)ethane. All bond lengths and angles within the two distinct types of pyrroles in **14** are nearly equivalent with the exception of the $C_\alpha-N_{pyrrole}-C_\alpha$ bond angles. The angles in pyrroles with the fused benzo rings (106.8(5)°) are larger than those in the sulfur-appended pyrroles (104.8(5)°). They are consistent with larger $C_\alpha-N_{pyrrole}-C_\alpha$ bond angles reported for M(pc) rather than those in Ni[pz(d)$_4$]. The porphyrazine core is planar to within 0.007 Å and contains a centrally-bound Ni(II) ion and two bis(triethylphosphine)-platinum moieties coordinated to the periphery in a trans geometry. The nickel atom lies on a crystallographic center of symmetry and the coordinated Ni−N bond lengths are 1.894-(5) Å and 1.879(5) Å to N(1) and N(15), respectively. The deviations from square-planar geometry are negligible; the N−Ni−N angles are 89.6(2) and 90.04(2)°. The planarity of the central core extends to include both thiolate sulfur atoms and the platinum centers, the maximum deviation from planarity being 0.08 Å for one of the sulfur atoms. As the structure is centrosymmetric there is only one independent Pt(II) position. The peripheral platinum(II) ions are coordinated by the P atoms of the two triethylphosphines and two macrocyclic S atoms in a roughly square-planar geometry. The P−Pt−P angle is noticeably enlarged at 97.47(6)° as a consequence of the bulky triethylphosphine substituents. The bite of the dithiolate moiety appears to be optimal, the S−Pt−S angle being 89.86(6)°. The Pt−P and Pt−S bond lengths (Pt−P(1) 2.286 (2); Pt−P(2) 2.293 (3); Pt−S(1) 2.333(3); Pt−S(2) 2.338(2) Å) are similar to those reported for related Pt(II) complexes having *trans* phosphorus and sulfur ligands.[10]

Table 4. Symmetry-Averaged Bond Distances and Bond Angles for *gemini*-Porphyrazines **14** and Related Macrocycles

	14	M(pc)[a]	[Ni(dppe)]$_4$[Ni(pzot)][b]
	Bond Distances (Å)[c]		
Ni−Np	1.886(5)	1.88(6)	1.87(3)
$C_\alpha-N_p$	1.384(8)	1.376(10)	1.41(1)
$C_\alpha-C_\beta$	1.448(8)	1.453(3)	1.46(3)
$C_\beta-C_\beta$	1.381(9)	1.395(4)	1.36(1)
$C_\alpha-N_m$	1.320(8)	1.328(7)	1.34(3)
$C_\beta-C_\gamma$	1.387(9)	1.394(2)	
$C_\gamma-C_\delta$	1.373(10)	1.385(7)	
$C_\delta-C_\delta$	1.383(11)	1.394(2)	
C_β−S	1.719(6)		1.71(1)
S···S	3.30		3.25
	Bond Angles (deg)[c]		
$C_\beta-C_\beta$−S	124.0(5)		123.5(5)
$C_\alpha-C_\beta$−S	129.2(5)		129.5(13)
$C_\alpha-C_\beta-C_\beta$	106.6(5)	106.7(3)	107.0(8)
$C_\alpha-N_p-C_\alpha$	105.8(5)	108.1(8)	103.5(7)
$N_m-C_a-N_p$	127.7(5)	127.7(1)	126.3(12)
$C_\alpha-N_m-C_\alpha$	120.3(5)	123.2(5)	120.8(19)
$N_p-C_\alpha-C_\beta$	110.6(5)	109.3(4)	110.0(14)
$N_m-C_\alpha-C_\beta$	121.7(6)	123.0(2)	122.8(17)
$C_\alpha-C_\beta-C_\gamma$	132.7(6)	132.2(2)	
$C_\beta-C_\beta-C_\gamma$	120.9(6)	121.3(2)	
$C_\beta-C_\gamma-C_\delta$	117.6(6)	117.3(2)	
$C_\gamma-C_\delta-C_\delta$	121.5(7)	121.6(1)	
Np−Ni−Np	90.0(2)	90	90.0(17)
Np−Ni−Np′	180.0(1)	180	178.1(1)

[a] Reference 8. [b] Reference 9. [c] Number in parentheses is the standard deviation in the last one or two digits of the values used in the symmetry average.

(7) (a) Fitzmaurice, J. C.; Slawin, A. M.; Williams, D. J.; Woollins, J. D.; Lindsay, A. J. *Polyhedron* **1990**, *9*, 1561−1565. (b) Bevilacqua, J. M.; Zuleta, J. A.; Eisenberg, R. *Inorg. Chem.* **1994**, *33*, 258−266.

(8) Schramm, C. J.; Scaringe, R. P.; Stojakovic, D. R.; Hoffman, B. M.; Ibers, J. A.; Marks, T. J. *J. Am. Chem. Soc.* **1980**, *102*, 6702−6713.

(9) Velazquez, C. S.; Baumann, T. F.; Olmstead, M. M.; Hope, H.; Barrett, A. G. M.; Hoffman, B. M. *J. Am. Chem. Soc.* **1993**, *115*, 9997−10003.

(10) (a) Bevilacqua, J. M.; Eisenberg, R. *Inorg. Chem.* **1994**, *33*, 2913−2923. (b) Chan, L. T.; Chen, H.-W.; Fackler, J. P.; Masters, A. F.; Pan, W.-H. *Inorg. Chem.* **1982**, *21*, 4291−4295. (c) Weigand, W.; Bosl, G.; Polborn, K. *Chem. Ber.* **1990**, *123*, 1339−1342. (d) Cavell, K. J.; Jin, H.; Skelton, B. W.; White, A. W. *J. Chem. Soc., Dalton Trans.* **1992**, 2923−2930.

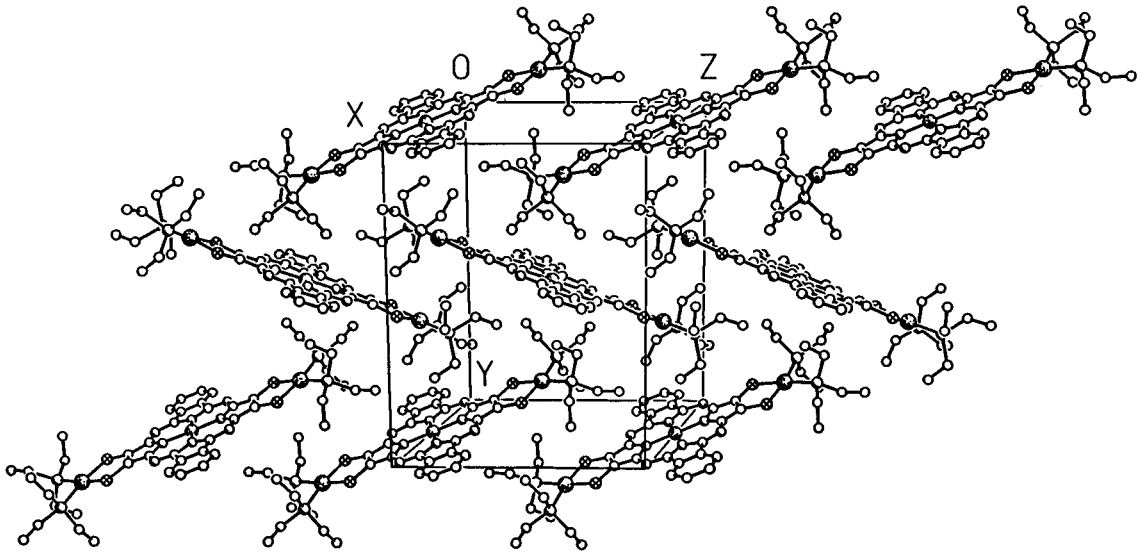

Figure 3. Packing diagram for complex **14**.

The intramolecular Ni···Pt and Pt···Pt distances are 7.18 and 14.36 Å, respectively. The nearest intermolecular Ni···Pt and Pt···Pt distances are shorter at 6.66 and 6.29 Å, respectively. The macrocycles pack in a slipped stack, "herring-bone" fashion (Figure 3), similar to that observed for Ni-phthalocyanine.[11] Here, however, the distance between neighboring parallel-aligned porphyrazines is much larger, the Ni···Ni separation being 13.01 Å (i.e., a lattice translation in the crystallographic *a* direction). The interplanar separation is 3.33 Å, but there is no $\pi-\pi$ overlap. It must therefore be concluded that the bulky triethylphosphine ligands disrupt potential intermolecular $\pi-\pi$ stacking forces.

Electronic Absorption Spectroscopy. Porphyrazines, like phthalocyanines, typically show an intense B (Soret) band at $\lambda < 400$ nm and a Q band that has its principal absorption at $\lambda > 600$ nm, with additional vibronic structure to shorter wavelength.[12] As seen with unsymmetrically-substituted phthalocyanines,[5] peripheral functionalization of a porphyrazine can significantly affect the electronic structure of the porphyrazine π-system, with this being most clearly seen in perturbations of the Q band. Gouterman's highly simplified four-orbital model[13] for porphyrinic macrocycles provides a qualitative description of the optical spectra of the M[pz(A_n:B_{4-n})] compounds (Figure 4). In a D_{4h}-symmetric macrocycle such as Ni(pc), the LUMO is doubly degenerate (e_g) and to a first approximation the Q and B bands are associated with transitions from the two highest occupied MOs (a_{1u}, a_{2u}) into the LUMO. This pattern is doubled in the lowered symmetry (D_{4h} to D_{2h}) of H_2(pc) with the splitting into two "0-0" (Q_x,Q_y) bands by 710 cm^{-1} being particularly clear.[14] The reduction in symmetry of the macrocycle removes the degeneracy of the e_g LUMO and gives rise to a split Q band. Likewise, visible spectra of the previously reported $n = 1$ porphyrazine, Ni[pz(a:b_3)], show a Q band with slightly split profile, presumably due to the lowered symmetry of the macrocyclic core from D_{4h} to C_{2v}.[2] Similar effects are seen in the optical spectra of the C_{2v}-symmetric $n = 3$ porphyrazine, **8**, whose optical spectrum resembles that of the C_{2v}-symmetric $n = 1$ porphyrazine, but with the transitions clearly broadened, due probably to the presence of underlying *n* to π^* transitions from the lone pairs on the six peripheral sulfur atoms (Figure 5).

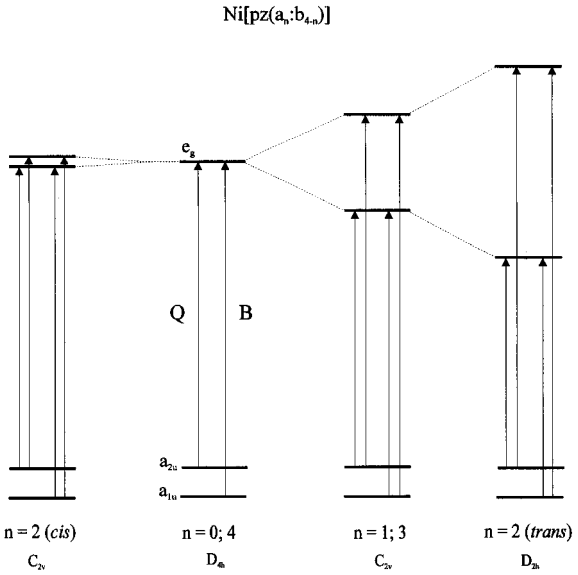

Figure 4. Qualitative orbital energy diagram for the Q and B (Soret) bands of the Ni[pz(a_n:b_{4-n})] porphyrazines, $n = 0-4$, showing the effect that the symmetry of the conjugated porphyrazine core has on the electronic structure of the macrocycle.

In the case of the $n = 2$ porphyrazines, the spectra of the *cis* and *trans* isomers are markedly different. Considering the D_{2h} symmetric *trans*-porphyrazines, splitting of the LUMOs (Figure 4) by the different substituents in the "*x*" and "*y*" directions of the porphyrazine core leads to large splittings of the Q band in the M[*trans*-pz(a_2:b_2)] porphyrazines, **5** (M = 2H), **9** (M = Ni), and **11** (M = Mn),[15] with quite distinct Q_x (605 nm for **9**; 654 nm for **11**) and Q_y (722 nm for **9**; 780 nm for **11**) transitions, Figure 5. The splittings of $\Delta E = 2680$ cm^{-1} for **9** and 2470 cm^{-1} for **11** are similar to that recently reported for a *trans*-substituted porphyrazine[3a] and nearly four times larger than those for H_2 (pc) or for unsymmetrically-substituted phthalocyanines.[3b,5] The reduction of symmetry is accentuated in the free-base *trans*-macrocycle, **5**, where the splitting of the Q band is 3560 cm^{-1} (transitions at 590 and 747 nm).

(11) Robertson, J. M.; Woodward, I. *J. Chem. Soc.* **1937**, 219−230.
(12) Stillman, M. J.; Nyokong, T. In *Phthalocyanines: Properties and Applications*; Leznoff, C. C., Lever, A. B. P., Eds.; VCH: New York, 1989; Chapter 3.
(13) (a) Gouterman, M. In *The Porphyrins*; Dolphin, D., Ed.; Academic Press: New York, 1978; Vol. III, pp 1−165. (b) Mack, J.; Kirkby, S.; Ough, E. A.; Stillman, M. J. *Inorg. Chem.* **1992**, *31*, 1717−1719. (c) Cory, M. G.; Hirose, H.; Zerner, M. C. *Inorg. Chem.* **1995**, *34*, 2969−2979. (d) Liang, X. L.; Flores, S.; Ellis, D. E.; Hoffman, B. M.; Musselman, R. L. *J. Chem. Phys.* **1991**, *95*, 403−417.
(14) Lever, A. B. P. *Adv. Inorg. Chem. Radiochem.* **1965**, *7*, 27−114.
(15) We ignore the axial ligand to Mn(III) in discussing symmetry.

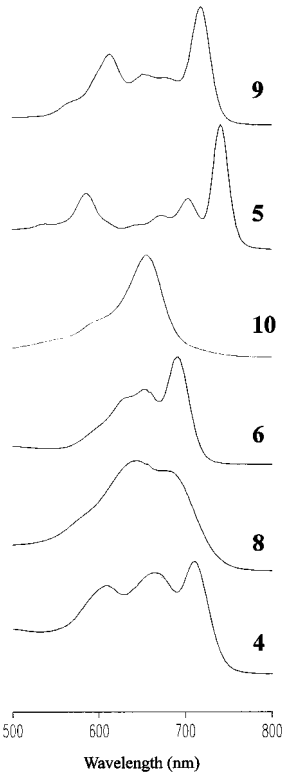

Figure 5. Electronic absorption spectra (in CH_2Cl_2) for the unsymmetrical 2H-, **4**−**6**, and Ni-porphyrazines, **8**−**10**.

In contrast, the C_{2v}-symmetric metalated $n = 2$ *cis*-porphyrazine isomers, **10** and **12**, show only a single Q band at 660 (Figure 5) and 712 nm, respectively, despite the fact that there are no doubly-degenerate representations in C_{2v}.[16] This apparent anomaly also can be explained within the four-orbital picture; the substituents along the "*x*" and "*y*" directions are, in fact, the same, so the LUMO remains accidentally degenerate (Figure 4), and there should be only a single Q band, as observed. Thus, this latter case is intriguingly equivalent to that seen in D_{4h} symmetric macrocycles. Not surprisingly, the metal-free *cis*-porphyrazine, **6**, shows a split Q-band. The further lowering of molecular symmetry of this macrocycle has removed the accidental degeneracy of the LUMO by the same amount as for H2 (pc), ~700 cm^{-1} (peaks at 652 and 692 nm).

Interestingly, upon coordination of the peripheral metal ions, both the *cis*- and *trans*-*gemini*-porphyrazines, **14** and **16**, show spectra similar to that of **6**, with a single Q band and additional vibronic features. The different molecular geometries of each isomer are no longer observable in their optical spectra. It thus appears that the peripheral metal-ion chelates interact with the porphyrazine ring to an extent similar to that of a fused benzene ring, and the LUMO remains accidentally degenerate, as it is by symmetry in the D_{4h} symmetric case. This same effect was seen in the optical spectra of the *solitaire* porphyrazine complexes.[2]

Electrochemistry of the $H_2[pz(a_n:b_{4-n})]$ Series. To further probe the effect of ring substituents and their symmetry on the electronic structure of the porphyrazine, the electrochemistry of the free-base macrocycles **3**−**7** was investigated. Phthalocyanines typically show two reversible ring reductions but no reversible oxidation processes. Each macrocycle in this series also showed two reversible waves that can be attributed to ring-centered reductions (Table 5). A comparison of the potentials of $H_2(pc)$[17] with those of the thioether-appended porphyrazines **3**−**7** shows that both $H_2(pc)$ and $H_2[pz(a:b_3)]$, **7**, have a similar pair of reduction potentials at ~ −1.2 and ~ −1.6 V versus the Fc^+/Fc couple, while the $n = 2$ *trans*, $n = 3$, and $n = 4$ compounds (**5**, **4**, and **3**, respectively) all show a pair of reductions at −0.8 and −1.2 V. Only the *cis*-macrocycle, **6**, has intermediate reduction potentials of −1.0 and −1.4 V. Within the limit (+1.5 V) allowed by the solvent (CH_2Cl_2), no oxidation processes associated with the ring were observed. Finally, no obvious correlation between the reduction potentials of the thioether-appended porphyrazines and their respective electronic spectra was observed.

Table 5. Comparison of Half-Wave Potentials[a] of the Ring Reductions (RR) for the Porphyrazine Series. $H_2[pz(a_n:b_{4-n})]$

macrocycle	$E_{1/2}$ (RR1) (V)	$E_{1/2}$ (RR2) (V)
$H_2(pc)$[b]	−1.20	−1.54
7, $n = 1$	−1.2	−1.6
6, $n = 2$ *cis*	−1.0	−1.4
5, $n = 2$ *trans*	−0.8	−1.2
4, $n = 3$	−0.8	−1.2
3, $n = 4$	−0.8	−1.2

[a] Half-wave potentials are reported versus (Fc^+/Fc) couple. Electrochemical experiments for **3**−**7** were performed in distilled CH_2Cl_2 with 0.1 M $TBAPF_6$ as the electrolyte using a Pt working electrode and a Ag/AgCl reference electrode. [b] Reference 17.

Conclusion

We have presented the synthesis and characterization of the binuclear solitaire porphyrazines[2] and of the trinuclear *cis*- and *trans*-*gemini*-porphyrazines. The preparation of the *gemini* compounds involves a general synthetic strategy that employs relatively inexpensive or easily prepared starting materials. The use of a dinitrile pair with disparate polarities allows for the selective purification of each porphyrazine $M[pz(a_n:b_{4-n})]$, $n = 0-4$, including the *cis* and *trans* $n = 2$ isomers. The *gemini*-porphyrazine, **14**, is the first structurally-characterized porphyrazine or phthalocyanine with a trans-type substitution pattern. The different molecular symmetries of the $n = 1-4$ protected precursors, **3**−**12**, have a profound effect on the electronic structure of each macrocycle. The approach described here allows for the preparation of a wide number of novel *gemini*-porphyrazines whose properties will be the subject of future reports.

Acknowledgment. This work was supported by the National Science Foundation (CHE-9408561) and the Wolfson Foundation (U.K.) for equipment. J.W.S. thanks the National Institutes of Health (GM14876) for their support.

Supporting Information Available: Tables of elemental analyses, crystal data and structure refinement, atomic coordinates and equivalent isotropic displacement parameters, bond lengths and angles, anisotropic displacement parameters, and hydrogen coordinates (8 pages). See any current masthead page for ordering and Internet access instructions.

JA961912X

(16) Cotton, F. A. *Chemical Applications of Group Theory*; J. Wiley & Sons: New York, 1990; Appendix IIA.

(17) Bottomley, L. A.; Chiou, W. J. H. *J. Electroanal. Chem.* **1986**, *198*, 331−346.